Ind. J. Pharm. Edu. Res., 2026; 60(4):1681-1695.
https://www.ijper.org

Original Article

Anti-Proliferative and Anti-Metastatic Effects of Conessine in Human Osteosarcoma Cells: *In vitro* and *in silico* Evidence Targeting MMP2 and MMP9

Hafiz A. Makeen[1], Mohammad Albratty[2,*]

[1]Pharmacy Practice Research Unit, Department of Pharmacy Practice, College of Pharmacy, Jazan University, Jazan, SAUDI ARABIA.
[2]Department of Pharmaceutical Chemistry and Pharmacognosy, College of Pharmacy, Jazan University, Jazan, SAUDI ARABIA.

ABSTRACT

Background: Osteosarcoma is a predominant bone cancer characterised by increased metastatic potential, rapid proliferation, and insufficient clinical prognosis, making it the leading cause of cancer-related morbidity. Finding novel plant-derived therapeutic agents capable of suppressing tumor development and metastasis is a necessary priority. **Objectives:** The present study demonstrates the potential anticancer and anti-metastatic activity of conessine against MG-63 osteosarcoma cells via various *in vitro* assays. The study intended to elucidate the mechanism underlying conessine's action through molecular analysis. **Materials and Methods:** Examining the cytotoxic effects of conessine on TNF-α-induced and uninduced MG-63 osteosarcoma cells is essential to determine the LC_{50} value, based on the results of the MTT assay. The antiproliferative effects of conessine were assessed using transwell migration, aggregation, wound healing, and clonogenic assays. The impact of conessine on the β-catenin signalling system and metalloproteinases was examined by indirect ELISA and molecular docking analysis. The tumor microenvironment was induced by TNF-α, which stimulates inflammation. **Results:** The LC_{50} value of conessine, estimated using cell viability assays, was 154.83 µg/mL MG-63 cells and 91.948 µg/mL for TNF-α-induced MG-63 cells. Conessine exhibited a significant reduction ($p<0.05$) in migratory and metastatic activities of osteosarcoma cells even under TNF-α-induced inflammatory conditions. Conessine treatment significantly reduced the relative β-catenin expression by 1.14 units/mg protein, compared with 1.35 units in untreated cells. *In silico* analysis revealed an effective binding of MMP2 and MMP9 to conessine, characterised by stable hydrogen bonding and hydrophobic interactions. **Conclusion:** These results demonstrated the significant cytotoxic, anti-proliferative, and anti-metastatic effects of conessine, suggesting a promising alternative medicine for osteosarcoma treatment.

Keywords: Anticancer, Cytotoxicity, Matrix Metalloproteinases (MMPs), MG-63, Molecular docking, Molecular docking, MTT assay, β-catenin.

Correspondence:
Dr. Mohammad Albratty
Department of Pharmaceutical Chemistry and Pharmacognosy, College of Pharmacy, Jazan University, Jazan, SAUDI ARABIA.
Email: malbratty@jazanu.edu.sa

Received: 27-02-2026;
Revised: 16-04-2026;
Accepted: 03-06-2026.

INTRODUCTION

Osteosarcoma, the most prevalent malignant bone tumor affecting children and adolescents, is caused by DNA damage and genetic instability, perhaps triggered by many environmental circumstances, as suggested by studies.[1] While the association between triggering factors and osteosarcoma has been partially established, the underlying mechanisms remain incompletely elucidated. Tumor metastasis encompasses a complex pattern of events, including uncontrolled proliferation, damage to the Extracellular Matrix (ECM), migration of neoplastic cells, and colonisation in distant body regions.[1] The metastatic dissemination of osteosarcoma cells, particularly to the lungs, is well documented as the principal cause of mortality in affected individuals.[2]

Matrix Metalloproteinases (MMPs) are one of the crucial molecular factors involved in tumor invasion and metastasis. MMPs are a cluster of endopeptidases that require calcium-zinc ions for enzymatic action and are able to interrupt all Basement Membrane (BM) and ECM molecules, including collagen I and IV, fibronectin, and laminin, in that way encouraging the cells to invade, migrate, and angiogenise.[3] Therefore, inhibiting MMP activity is emerging as an essential strategy for reducing tumor growth and metastatic dissemination. The Wnt/β-catenin signalling is another crucial pathway associated with metastasis. β-catenin operates the transcriptional regulation of gene expression that contributes to metastatic traits.[4] Thus, targeting

DOI: 10.5530/ijper.20264949

β-catenin signalling poses a promising approach for the development of innovative antitumor therapeutics.

Despite the advances in chemotherapy and surgical interventions, the likelihood of survival for osteosarcoma remains poor, especially in metastatic instances, highlighting the urgency to develop a novel anticancer drug possessing anti-metastatic features.[5] Conessine is one of the C-24 steroid alkaloids found in bark and seeds of plants in the Apocynaceae family, widely used as traditional medicine.[6] Its exhibits lipophilic characteristics that facilitate membrane permeability and interaction with intracellular molecular targets.[7] Although conessine has been reported to exhibit anti-inflammatory and anticancer abilities, the antimetastatic effects of conessine in osteosarcoma and other types of cancers remain, to the best of our knowledge, scarcely explored. Consequently, this work aimed to examine the anticancer and antimetastatic properties of conessine in MG-63 osteosarcoma cells under TNF-α-induced Tumor Microenvironment (TME). The inhibitory effects of conessine on cancer cell survival, motility, colony formation, and cell aggregation were assessed via various *in vitro* tests. The role of β-catenin signalling was assessed using an indirect ELISA test. Additionally, molecular docking analysis was conducted to assess the potential interaction between conessine and Metastasis-Associated Enzymes (MMPs), offering mechanistic insights into its antimetastatic properties.

MATERIALS AND METHODS

Preparation of Chemicals and Cell line

MG-63 (Human Osteosarcoma) cell line was obtained from the ATCC and maintained in Dulbecco's modified Eagle's medium (Sigma Aldrich, USA). Conessine and TNF-α were procured from (Sigma, M-5655). Conessine and DMSO (0.1%) were mixed in a 1:1 ratio using a cyclomixer and sterilised by a Millipore syringe filter (0.22 µm). 15 mg of 3-(4,5-dimethylthiazol-2-yl)-2,5-diphenyl tetrazolium bromide (MTT) (Sigma, M-5655) was reconstituted in 3 mL PBS and sterilised before use. Varying conessine concentrations, including 6.25, 12.5, 25, 50, and 100 µg/mL, were prepared for further analyses. MG-63 cell line was raised in DMEM supplemented with FBS (10%), L-glutamine, sodium bicarbonate, and antibiotics (Penicillin, Streptomycin, and Amphotericin B) and sustained at 37°C in 5% CO_2 incubator. Cell viability was frequently assessed by MTT assay.[8] For analyses, a two-day-old confluent monolayer of cells was trypsinised and suspended in growth medium (10%). 100 µL cell suspension containing $5x10^3$ cells/well was seeded in the tissue culture plate and incubated at 37°C for the assays.

Cytotoxicity Assay

The cytotoxic activity of conessine on MG-63 human osteosarcoma cells was evaluated using microscopy and MTT assay. Varying concentrations (6.25, 12.5, 25, 50, and 100 µg/mL) of freshly prepared conessine compounds were added to the 96-well plate loaded with MG-63 $5x10^3$ cells/well, except to the control.[9] After incubation at 37°C in a humidified 5% CO_2 incubator for 24 hr, the entire plate was observed in an inverted phase-contrast tissue culture microscope (Olympus CKX41 with Optika Pro5 CCD camera), and images were recorded.

Quantitative evaluation of cytotoxicity exhibited by conessine was performed by MTT assay. 30 µL of reconstituted MTT solution was added to all the test and control wells. After 4 hr of incubation, 100 µL of Dimethyl sulphoxide was used to solubilise the formazan crystals, and the Optical Density (OD) was read using a microplate reader at a wavelength of 540 nm.[10] The percentage of growth inhibition was calculated using the formula:

Percentage of viability = (Mean OD Samples X 100)/Mean OD of the control group

Effect of Conessine on TNF-α-Induced MG-63 Cells

Cytotoxic assay was performed to evaluate the modulatory effect of conessine on MG-63 cells under TME.[11] TME was mimicked by TNF-α (2 pg/mL), which was added to the MG-63 cell suspension ($5x10^3$ cells/well) in a 96-well plate and incubated for 48 hr. Freshly prepared conessine at concentrations of 6.25, 12.5, 25, 50, and 100 µg/mL was added to evaluate the LC_{50}. An untreated control and TNF-α-induced MG-63 cells were maintained as well. After 24 hr incubation, the entire plate was subjected to microscopy and MTT assay to determine the cytotoxicity and modulation of structural damage exhibited by conessine in TNF-α-induced cancer cells.

Transwell Migration Assay

The transwell migration assay measures cell chemotaxis through a porous membrane by establishing a chemoattractant gradient using two medium-filled compartments. Trypsinized MG-63 cells ($2x10^5$) were loaded into a 12-well plate and incubated for 24 hr to attain 90% confluency. Cells were induced with TNF-α and further treated with conessine (91.948 µg/mL) as described in the cytotoxicity assay. Wells maintained with a control (MG-63 untreated), TNF-α-induced, TNF-α-induced and treated with conessine, and uninduced MG-63 treated with conessine, to evaluate the anti-migratory effect of conessine under TME. After 24 hr, 0.25% trypsin-EDTA was added to detach the cells from the tissue culture plate, and the precipitated cells were resuspended in serum-free media. The filter membrane in a transwell insert was added with a 100 µL aliquot and incubated for 10 min at 37°C. 600 µL of DMEM with FBS (10%) was loaded into the lower chamber and incubated for 24 hr. Non-migrated cells from the membrane were removed using a cotton-tipped applicator, and the migrated cells in the transwell insert were fixed with ethanol (70%), followed by drying. The migrated MG-63 cells, attached to the underside of the membrane, stained with crystal violet (0.2%), were counted under an inverted microscope.[12]

Clonogenic Assay

Clonogenic assay is used to measure the ability of cells to grow in anchorage-independent manner and form colonies. Trypsinised MG-63 cell suspension was induced with TNF-α and treated with conessine as described in the previous assay. Clonogenic assay was performed in 6-wellplate, in which the bottom layer was formed with 2 mL of agarose (1%) mixed with DMEM (1:1). Followed by solidification, the top layer was formed by 2 mL of agarose (0.8%)-DMEM mix made with the ratio 5:6. After 15 min of solidification, the above transfected cell suspension was spread on to the medium and incubated for 14 days for colony formation.[13] Formaldehyde (4%) and Crystal violet (0.005%) stained colonies were counted and recorded.

Scratch Wound Healing Assay

The impact of conessine on the migratory potential of MG-63 cells was determined using a scratch wound healing assay in 12-well plates. Trypsinised MG-63 cell suspension was induced with TNF-α and treated with conessine as described in the previous assay. The scratch wound was created using a sterile 1 mL pipette tip through a pre-marked line on the cancer cell line ($2x10^5$) maintained with ∼90% confluency. After five lineal scratches, debris was removed, and the monolayer was washed in PBS prior to treating with conessine (IC_{50}) and incubated for 0, 24, 48 and 72 hr. Wound closure was observed microscopically at 0, 24, 48, and 72 hr of incubation and quantitatively measured using MRI-Image J analysis software.[14]

Cell Aggregation Assay

Qualitative analysis of MG-63 cell aggregation after conessine treatment was evaluated by a semi-solid agar cell aggregation assay.[15] 100 µL of TNF-α-induced conessine-treated cell suspension, washed with Moscona solution (3 mL), was added onto the solidified agar solution (Bacto-agar, procured from Difco Laboratories, Detroit, MI, USA) (40-50°C) in 96-well microtiter plates. Cells are gently mixed to ensure uniform application and incubated at 37°C in a humidified atmosphere. The aggregates were fixed with formaldehyde (4%) and stained with crystal violet (0.005%) and observed under a microscope at the time intervals of 24, 48, and 72 hr.

Indirect ELISA for relative β-Catenin Expression

Indirect ELISA quantitatively measures the expression level of β-catenin in osteosarcoma cells induced with TNF-α and evaluates the impact of conessine on it. 100 µL of TNF-α-induced and conessine-treated cell suspension was seeded into microtiter plates and incubated. The assay was conducted according to the protocol described by Surendran *et al.*[16] 100 µL of β-catenin was used as primary antibody (1:500 dilution), and an equal amount of HRP-conjugated secondary antibody was used. OD was measured at 415 nm using an ELISA reader. Total protein concentration was determined using Bradford.[17] Absorbance was read at 595 nm (UV-VIS Spectrophotometer- SHIMADZU-UV-1900i), and protein concentration was calculated using the standard curve. The β-catenin protein level was calculated using the following formula:

$$\text{Relative β-catenin expression} = \text{OD value/Total protein concentration}$$

Molecular Docking Study of Conessine with MMPs

Preparation of the Target proteins

The three-dimensional X-ray crystallographic structures of matrix MMPs (MMP9 and MMP2) were retrieved from the Research Collaboratory for Structural Bioinformatics Protein Data Bank (RCSB-PDB) (http://www.rcsb.org/pdb/home/home.do). The proteins were corrected (Biovia Discovery Studio v.25) by inserting missing atoms and loop regions and removing water molecules and conformations. Atom names standardisation, titratable residues protonation using predicted pKa values, and energy minimisation were performed prior to docking analysis.

Preparation of Ligands

The chemical structure of conessine was retrieved from PubChem compound database (https://pubchem.ncbi.nlm.nih.gov/). The retrieved ligand structure comprises different protonation states and 3D geometries, and further optimising them by editing and generating favourable variations suitable for the docking study.

Molecular Docking Analysis

The molecular interaction between the MMPs (target) and conessine (ligand) was studied using Biovia Discovery Studio v.25. The binding sites of MMPs were predicted using the tool 'define and edit binding site' available in the software on the basis of PDB site records. The LibDock protocol, which provides a high-throughput docking algorithm to recognise polar interaction hotspots in ligand binding, assisted in studying molecular interactions.[18] The CHARMM force field was applied to learn the positional relationships between atoms and calculate the intermolecular interactions. Ligand-protein complexes, generated from the multiple docking poses, were evaluated based on LibDock scores and binding energies. The favourable docking conformations were selected and analysed to identify hydrogen-bonding, hydrophobic interactions, and interacting amino acid residues that stabilise the MMP-conessine complexes.

Statistical Analysis

All experiments were performed in triplicate as independent biological replicates, with each condition tested in parallel wells. The resulting outcomes were given as Mean±SD, and the values were analysed for statistical comparison using Graphpad PRISM 5.1. The values were subjected to one-way ANOVA, and the groups were compared using Tukey's multiple comparison test. $p<0.05$, $p<0.01$, and $p<0.001$ denote varying degrees of

statistical significance, categorised as statistically significant, very significant, and extremely significant, respectively, where applicable.

RESULTS

Cell Viability Assay

The cytotoxic effect of conessine on MG-63 human osteosarcoma cells was assessed using microscopy and MTT assay. Figures 1A-1F shows images captured by a phase-contrast tissue culture microscope, indicating dosage-dependent cytotoxicity in conessine-treated cells compared to the untreated osteosarcoma cells. The untreated control cells of osteosarcoma exhibited a spindle-shaped cell morphology with an intact cell membrane and strong adherence to the culture surface Figure 1A. Treatment with conessine induces morphological variations that are favourable to cytotoxicity. The low dosage of conessine showed mild structural variations Figures 1B-1D, including compact cell concentration, rounding, shrinking and incomplete adherence. At higher doses, widespread structural damage was apparent, including cell shrinkage, complete reduction of adherence, and formation of cellular debris Figures 1E and F. Conessine exhibited a dose-dependent reduction in cell viability Figure 1G. The lowest tested concentration of conessine, 6.25 µg/mL showed the maximum viability of 97.29± 0.10% compared to the control, exhibiting low cytotoxicity. 100 µg/mL conessine exhibited a viability of 68.35±0.47%, comparatively higher. The LC_{50} value was estimated using a standard dose-response curve analysis based on the percentage cell viability. Although the highest tested concentration (100 µg/mL) did not reach 50% inhibition in normal MG-63 cells, the regression model allowed extrapolation of the LC_{50} value (154.83 µg/mL) based on the observed dose-response trend.

Modulatory Effect of Conessine on TNF-α-Induced Cellular Stress

The MTT assay results demonstrated the cytotoxic effect of conessine at varying concentrations on MG-63 cells under TNF-α-stimulated TME. Phase-contrast microscopy was initially used to examine the morphological variations, followed by quantitative analysis to determine cell viability Figure 2A. TNF-α-induced cells Figure 2B exhibited noticeable morphological alterations, including cell rounding, loss of adhesion, and reduced cell density compared to control (MG-63 cells), indicating cellular stress. Treatment with conessine resulted in dose-dependent cytotoxicity along with comparatively improved structural integrity (Figures

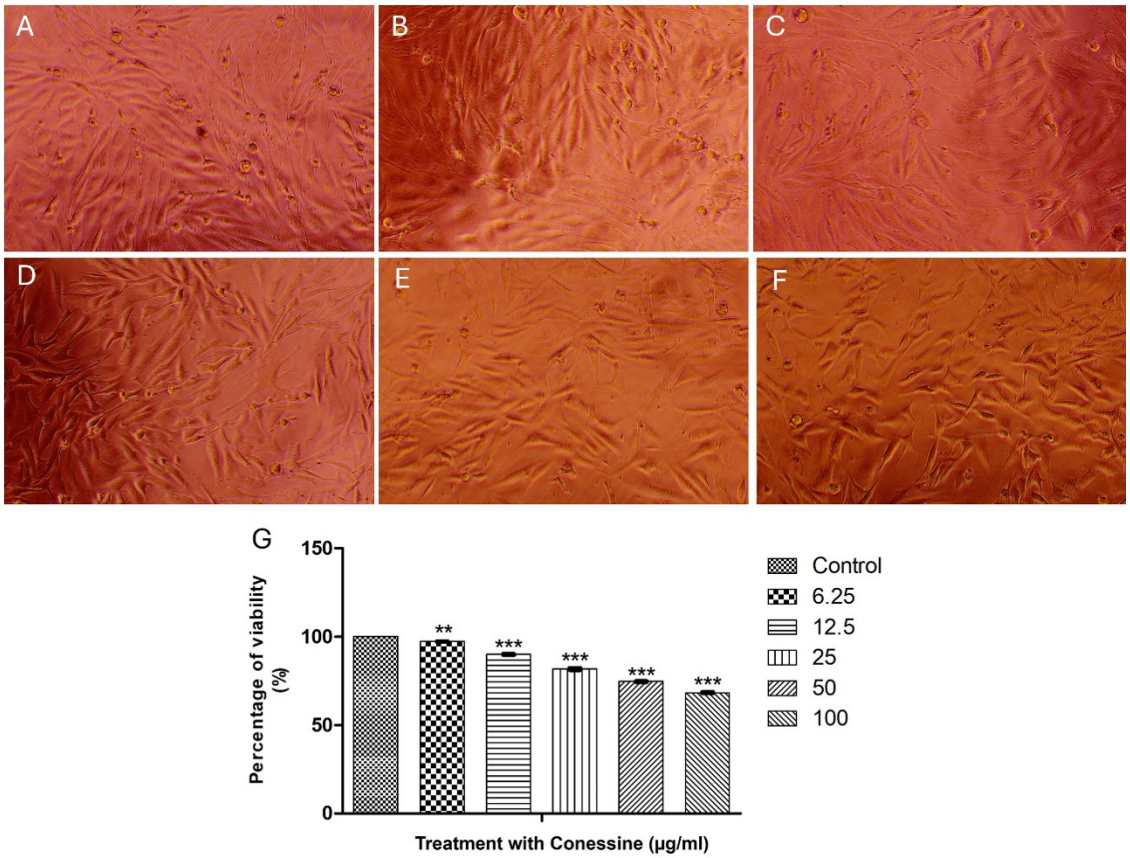

Figure 1: Effect of conessine on the viability of MG-63 osteosarcoma cells assessed by MTT assay. MG-63 cells were treated with varying concentrations of conessine for 24 hr. Conessine significantly reduced the cell viability with an LC_{50} of 154.83 µg/mL. A-F: Microscopic observations depicting detectable changes in the morphology of the cells. A-Control; B-6.25; C-12.5; D-25; E-50; and F-100 µg/mL. G - Graphical representation showing the dose-dependent inhibition of conessine on MG-63 cells. All experiments were performed in triplicate, and data are expressed as Mean±SE. Statistical analysis was performed using one-way ANOVA followed by Dunnett's test. $^{**}p<0.01$, $^{***}p<0.001$ compared to control.

2C-2G). Conessine treatment reduced cellular debris formation and partially restored the morphology of TNF-α-induced cancer cells compared to untreated cells Figure 2B. This finding suggests that conessine treatment not only reduced the cell viability but also attenuated/modulated the morphological abnormalities induced by TNF-α. Graphical representation further confirmed a significant reduction in cancer cell viability in a dose-dependent manner, with 6.25 - 100 µg/mL of conessine exhibiting the viability ranging from 87.75 - 47.46%, respectively (Figure 2H). Statistical analysis revealed that the reduction in cancer cell viability was highly significant (***p<0.001) compared to the untreated group. TNF-α-induced cells reached near 50% inhibition within the tested range, resulting in a more directly supported LC_{50} value, 91.94 µg/mL.

Transwell Migration Assay

TNF-α-increased the migratory potential of MG-63 cells compared to the uninduced control group. Figures 3A-3D show the microscopic images of crystal violet-stained transwell membrane, showing migrated cells towards the chemoattractant. The membrane of the control group showed significantly dense cells, indicating elevated migratory activity Figure 3A, with 819 cells. TNF-α-induced MG-63 cells appear aggregated, highly dense, indicating more aggressive migratory activity (894 cells), Figure 3B. Conessine treatment significantly reduced migratory activity, as there was no aggregation, and cells (348 cells) were not dense, with high clear zones of the membrane visible. However Figure 3D shows that conessine does not affect the migration of normal MG-63 cells due to the absence of metastatic effect. These results demonstrate the anti-migratory effect of conessine on osteosarcoma cells under TME.

Clonogenic Assay

Subsequent treatments and colony formation show a single cell's capacity to preserve its propagative integrity and yield a clonogenic colony. The control group shows a high intensity of dye, indicating substantial cell count Figure 4A. The well comprising osteosarcoma cells induced with TNF-α showed very high intensity compared with the control, indicating stimulation of proliferative signals that lead to the tumor cell's clonogenic survival (Figure 4B). These results were confirmed by recording 98 colonies from TNF-α-induced untreated cells, the highest among the others Figure 4E. Conessine treatment significantly inhibited the clonogenic survival of tumor cells, as a low density of stained cells was observed from the wells, and the count of colonies was 14, significantly lower when compared to the untreated cells. Conessine treated to the MG-63 cells exhibited 26

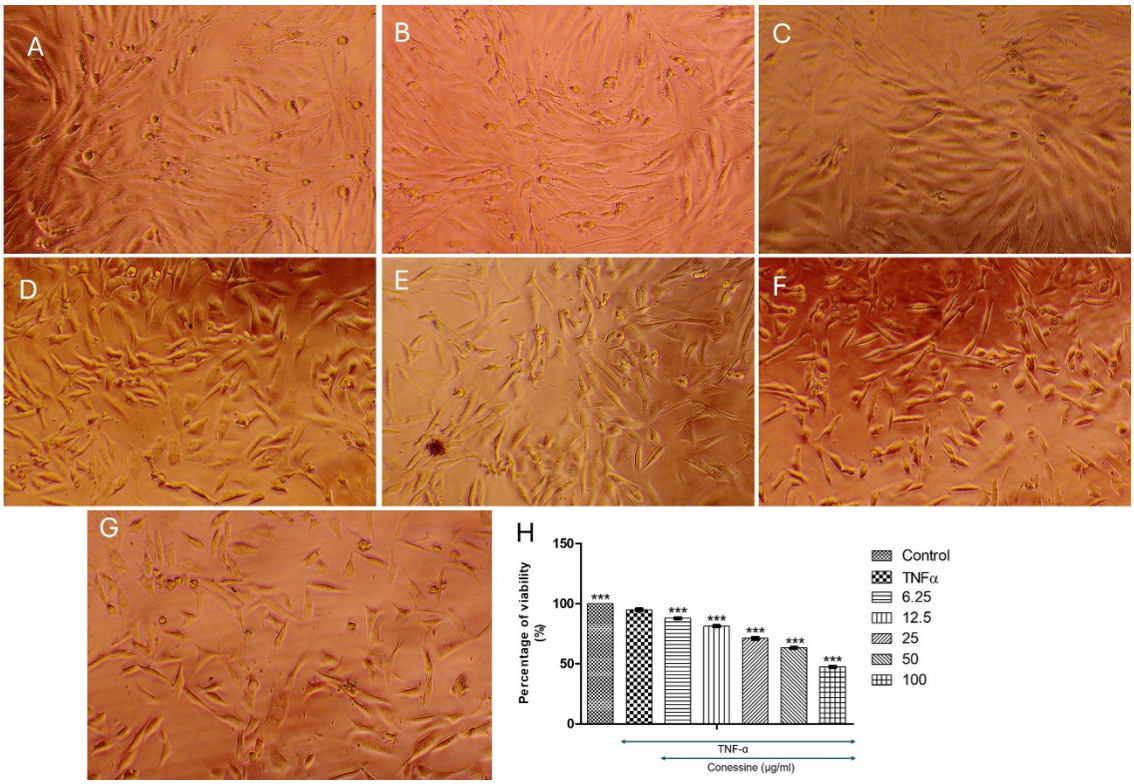

Figure 2: Effect of conessine on the viability of TNF-α-induced osteosarcoma cells (MG-63) assessed by MTT assay. TNF-α-induced MG-63 cells were treated with varying concentrations of conessine for 24 hr. Conessine significantly reduced the cell viability with an LC_{50} of 91.948 µg/mL. A-G: Microscopic observations depicting detectable changes in the morphology of the cells. A-Control; B-G are TNF-α-induced and treated using 0, 6.25, 12.5, 25, 50, and 100 µg/mL respectively. H - Graphical representation showing the dose-dependent inhibition of conessine on TNF-α-induced MG-63 cells. All experiments were performed in triplicate, and data are expressed as Mean±SE. Statistical analysis was performed using one-way ANOVA followed by Dunnett's test. **p<0.01, ***p<0.001 compared to control.

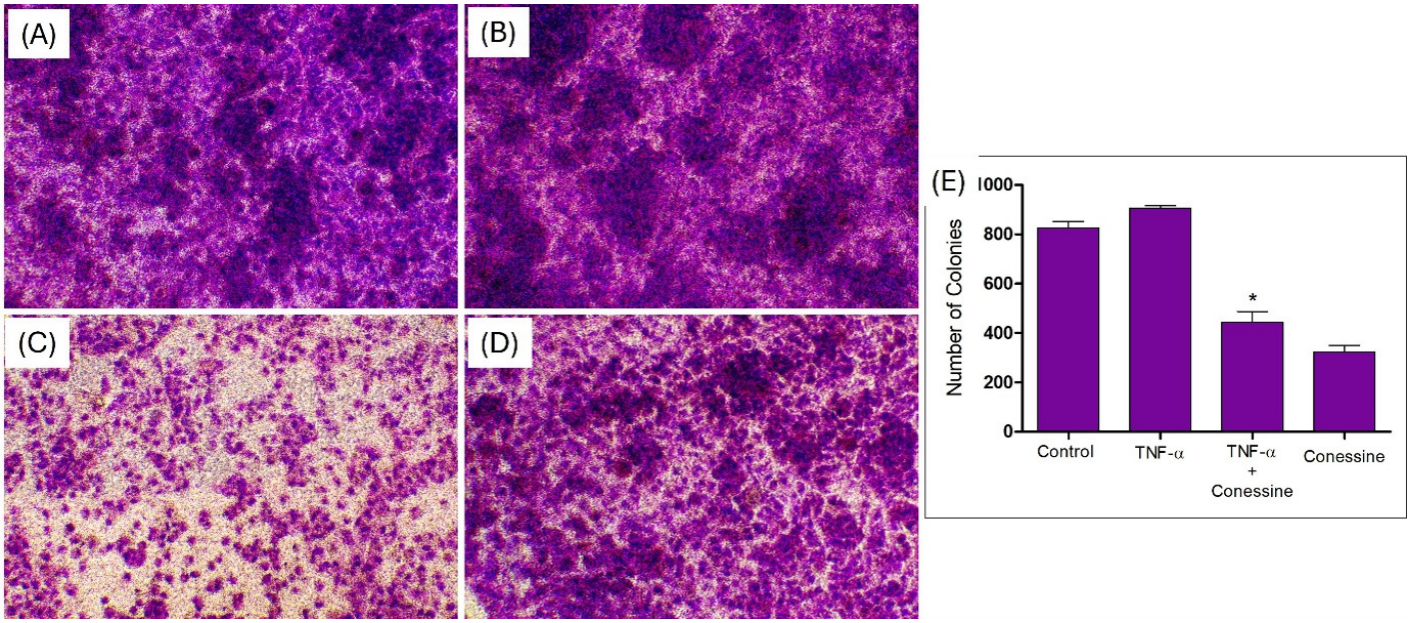

Figure 3: Effect of conessine on migration of MG-63 osteosarcoma cells assessed by transwell migration assay. A-C: Inverted microscopic images of crystal violet-stained transwell membrane. A-Untreated MG-63 cells (Control); B-TNFα-induced; C-TNFα-induced cells treated with conessine; D-Conessine treated healthy MG-63 cells; E-Graphical representation depicting the number of colonies observed from the transwell membrane. Conessine markedly suppressed TNF-α-induced migration. *p<0.05 versus control.

colonies, which showed the absence of anti-clonogenic efficacy of conessine on normal MG-63 cells Figures 4C-4E.

Scratch Wound Assay

The control group, with untreated MG-63 cells, showed normal progressive wound closure, with the scratch area decreasing to 814,854 px at 24 hr to 0 px by 48 hr. In TNF-α-induced group, the cells exhibit more active migration than non-metastatic MG-63 cells, achieving a wound area of 1,039,042 px in 24 hr and complete closure by 48 hr. In contrast, treatment of TNF-α-induced MG-63 cells using conessine inhibited wound closure, and the wound area remained open until 72 hr. The wound area values for conessine-treated MG-63 cells under TME were 1,607,970 px, 1,585,332 px, and 1,540,560 px at 24, 48, and 72 hr, respectively. Similarly, reduced migratory capacity and inhibition of wound healing were observed in conessine-treated MG-63 cells (not TNF-α-induced), in which the wound area was 1,226,838 px at 72 hr Figure 5.

Cell Aggregation Assay

The effect of conessine on the aggregation behaviour of MG-63 osteosarcoma cells for the different time periods was illustrated in Figure 6. After 24 hr of incubation, both the control group and TNF-α-induced MG-63 cells formed small to moderately compact cell aggregates, and the density was increasing, and large clusters were formed after 48 hr, indicating cell-cell interaction and aggregation capacity exhibited by osteosarcoma cells. In contrast, treatment with conessine markedly reduced aggregate formation and showed a few small and loosely arranged aggregates after 24 hr. Conessine treatment resulted in reduced aggregate size and number compared to control cells. Scattered and poorly organised cell clusters in conessine-treated TNF-α-induced MG-63 cells demonstrated the suppression of anchorage-independent cell-cell interaction, which is higher than that of conessine-treated MG-63 cells, which are not induced with TNF-α.

Indirect Elisa for β-Catenin Expression

As shown in Figure 7, upon stimulation with TNF-α, a marked increase in β-catenin activity was observed (1.35 units/mg protein), indicating activation of β-catenin signalling in MG-63 cells under inflammatory conditions. Treatment with conessine significantly reduced β-catenin activity in TNF-α-induced cells, with the activity decreased to 1.14 units/mg protein, demonstrating partial suppression of TNF-α-induced β-catenin expression. The lowest β-catenin activity (0.94 units/mg protein) was recorded in osteosarcoma cells treated with conessine. Conessine treatment exhibited a significant reduction in β-catenin activity compared to untreated TNF-α induced MG-63 cells, indicating the downregulation of β-catenin signalling in MG-63 osteosarcoma cells.

Docking Interaction Between Conessine and MMPs

The active site of the protein interacting with the standard drug was selected as the binding site. Molecular docking was performed using the LibDock module, generating a total of 30 docked poses for the selected ligands within the defined binding site of MMP9 and MMP2. The binding affinities of these ligands were evaluated based on LibDock scores, which reflect the geometric and energetic compatibility of the ligand within the receptor binding pocket. The molecular docking analysis evaluated the binding

Table 1: Interactions between MMP9 with Conessine and standard drug Batimastat.

Ligands	LibDock Score	Interacting Residue	Bond Distance	Bond Nature
Conessine (PubChem ID: 441082)	130.527	441082:H58 - A:ALA189:O	2.02834	Hydrogen Bond
		441082:H60 - A:ARG249:O	2.59051	Hydrogen Bond
		441082:H61 - A:ARG249:O	2.5605	Hydrogen Bond
		441082:H62 - A:ARG249:O	2.68651	Hydrogen Bond
		A:LEU188 - 441082	4.68818	Hydrophobic
		A:LEU188 - 441082	5.42503	Hydrophobic
		A:LEU222 - 441082	4.35906	Hydrophobic
		A:VAL223 - 441082	4.41368	Hydrophobic
		A:LEU243 - 441082	5.01804	Hydrophobic
		A:ARG249 - 441082	5.15202	Hydrophobic
		441082:C19 - A:LEU187	4.67801	Hydrophobic
		441082:C19 - A:LEU188	4.78935	Hydrophobic
		441082:C20 - A:LEU243	4.6005	Hydrophobic
		A:HIS226 - 441082	5.17549	Hydrophobic
		A:HIS226 - 441082	4.49693	Hydrophobic
		A:HIS226 - 441082	4.1983	Hydrophobic
		A:HIS226 - 441082:C20	4.09953	Hydrophobic
		A:TYR248 - 441082	4.82376	Hydrophobic
Batimastat (PubChem ID:5362422)	151.393	A:HIS226:HE2 - 5362422:O3	2.83451	Hydrogen Bond
		A:GLN227:HE21 - 5362422:O4	2.041	Hydrogen Bond
		5362422:H36 - 5362422:O3	2.10719	Hydrogen Bond
		A:VAL223:HA - 5362422:O4	2.67769	Hydrogen Bond
		A:HIS226:HD2 - 5362422:O4	2.78146	Hydrogen Bond
		5362422:H50 - A:ALA189:O	2.70128	Hydrogen Bond
		5362422:H40 - A:HIS226	2.46294	Hydrophobic
		A:HIS226 - 5362422	5.97015	Hydrophobic
		5362422:C13 - A:LEU188	4.27405	Hydrophobic
		A:HIS236 - 5362422:C29	4.68974	Hydrophobic
		5362422 - A:LEU222	5.35104	Hydrophobic
		5362422 - A:LEU243	4.93133	Hydrophobic
		5362422 - A:ARG249	4.91732	Hydrophobic

interactions of Conessine (PubChem ID: 441082) relative to the reference inhibitor Batimastat (PubChem ID: 5362422) using the LibDock scoring function.

MMP9 Docking with Conessine

The three-dimensional structure of MMP9 in complex with inhibitor BE4 was downloaded from the PDB database (PDB ID: 6ESM) with a crystallographic resolution of 1.10 Å. The protein consists of a polypeptide chain A with 160 amino acids. Conessine exhibited a LibDock score of 130.527, indicating a favourable binding affinity within the active site of the target protein. The binding was stabilised by multiple hydrogen bond interactions, notably with residues ALA189 and ARG249, with bond distances ranging from approximately 2.02 to 2.69 Å, suggesting strong and specific polar interactions. The hydrophobic interactions were also observed with residues such as LEU187, LEU188, LEU222, LEU243, VAL223, HIS226, and TYR248, which likely contribute to the overall stability of the ligand-protein complex Figure 8. The interacting residues, nature of the interacting bond and the bond distance are tabulated Table 1.

Batimastat (LibDock score: 151.393), used as the reference inhibitor and consistent with its well-established inhibitory potency, formed more hydrogen bonds with key active-site residues, including HIS226, GLN227, VAL223, and ALA189, with most bond distances below 3.0 Å, indicating strong interaction strength. In addition, Batimastat exhibited robust hydrophobic interactions with LEU188, LEU222, LEU243, and ARG249, thereby enhancing its binding efficiency within the catalytic pocket. These results show that conessine has the potential to interact moderately and exhibit favourable binding interaction

with the MMP9, although its binding affinity appears inferior to that of the standard inhibitor.

MMP2 Docking with Conessine

The three-dimensional structure of MMP2 catalytic domain in complex with inhibitor was downloaded from the PDB database (PDB ID: 7XGJ) and crystallographic resolution 2.80 Å. The protein consists of three polypeptide chain A, B and C, with 168 amino acids. The docked complex was analysed to study non-bond interactions between the target and the ligand. Conessine exhibited a LibDock score of 129.451, indicating a favourable binding affinity within the active site of the target protein. The binding was stabilised by multiple hydrogen-bond interactions, notably with residues ALA84 and THR144, with bond distances ranging from approximately 2.19 to 2.52 Å, suggesting strong, specific polar interactions. The hydrophobic interactions were also observed with residues such as LEU83, VAL118, ALA140, TYR143 and HIS121, which likely contribute to the overall stability of the ligand-protein complex Figure 9. The interacting residues, nature of the interacting bond and the bond distance are tabulated Table 2.

Batimastat (LibDock score: 151.363), used as the reference inhibitor and consistent with its well-established inhibitory potency, formed more hydrogen bonds with key active-site residues, including LEU83, ALA84, and GLY81, with most bond distances below 3.0 Å, indicating strong interactions. In addition, Batimastat exhibited robust hydrophobic interactions with HIS121, LEU83, HIS125 and VAL118, thereby enhancing its binding efficiency within the catalytic pocket. These results show that conessine has the potential to interact effectively with the MMP2, supporting its consideration as a lead compound, although its binding affinity appears lower than that of the standard inhibitor.

Table 2: Interactions between MMP2 with Conessine and standard drug.

Ligands	LibDock Score	Interacting Residue	Bond Distance	Bond Nature
Conessine (PubChem ID: 441082)	129.451	441082:H41 - A:ALA84:O	2.52599	Hydrogen Bond
		441082:H62 - A:THR144:O	2.30062	Hydrogen Bond
		441082:H63 - A:THR144:O	2.19751	Hydrogen Bond
		441082:H31 - A:HIS121	2.59393	Hydrophobic
		A:LEU83 - 441082	5.10672	Hydrophobic
		A:VAL118 - 441082	4.14168	Hydrophobic
		A:ALA140 - 441082	5.00146	Hydrophobic
		441082 - A:LEU83	4.99046	Hydrophobic
		441082:C20 - A:LEU138	4.6177	Hydrophobic
		A:HIS121 - 441082	4.51869	Hydrophobic
		A:HIS121 - 441082	4.57466	Hydrophobic
		A:HIS121 - 441082:C20	4.07829	Hydrophobic
		A:TYR143 - 441082	5.21217	Hydrophobic
Batimastat (PubChem ID:5362422)	151.363	A:LEU83:HN - 5362422:O4	1.87482	Hydrogen Bond
		A:ALA84:HN - 5362422:O4	2.49384	Hydrogen Bond
		5362422:H33 - A:GLY81:O	1.80604	Hydrogen Bond
		5362422:H34 - 5362422:O4	2.40136	Hydrogen Bond
		5362422:H36 - 5362422:O4	2.87863	Hydrogen Bond
		5362422:H36 - 5362422:O5	2.78875	Hydrogen Bond
		5362422:H59 - A:PRO141:O	2.6081	Hydrogen Bond
		5362422:H60 - 5362422:O5	2.52282	Hydrogen Bond
		5362422:S2 - A:HIS85	4.29962	Other
		A:HIS121 - 5362422	4.82221	Hydrophobic
		5362422:C29 - A:LEU83	4.3106	Hydrophobic
		A:HIS121 - 5362422:C13	4.67082	Hydrophobic
		A:HIS125 - 5362422:C13	4.07821	Hydrophobic
		5362422 - A:LEU82	4.69574	Hydrophobic
		5362422 - A:VAL118	5.32689	Hydrophobic

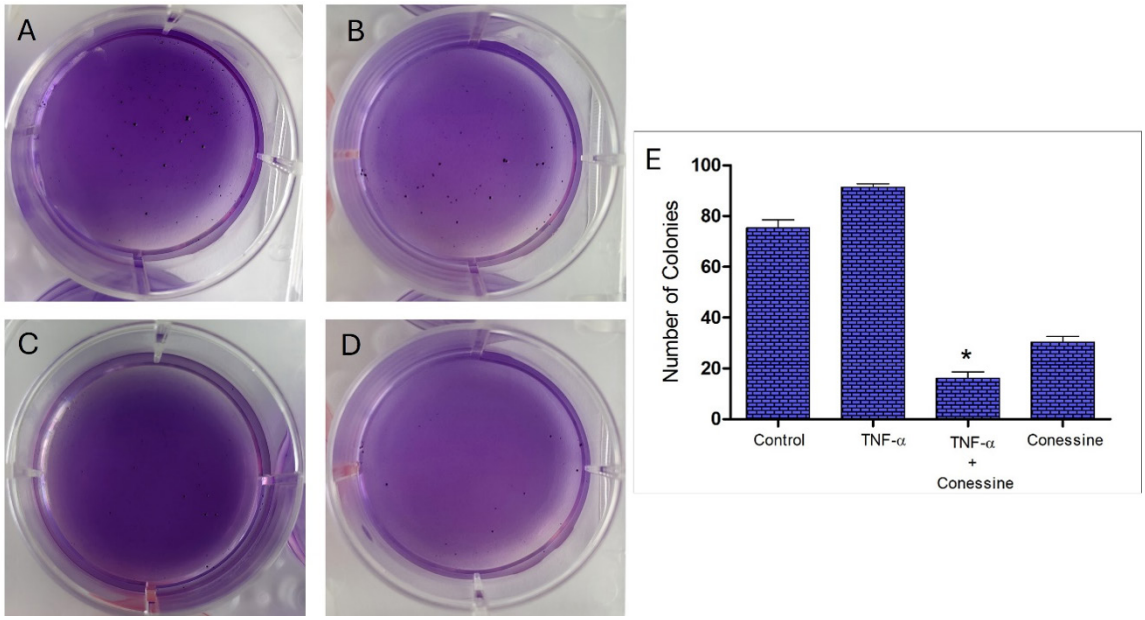

Figure 4: Effect of conessine on colony formation ability of osteosarcoma cells evaluated using clonogenic assay in 6-well plate. A-Untreated MG-63 cells (Control); B-TNFα-induced; C-TNFα-induced cells treated with conessine; D-Conessine-treated healthy MG-63 cells; E-Graphical representation depicting the number of colonies observed from the 6-well plate assay after 14-days. Conessine treatment significantly reduced colony formation both in TNF-α-induced and healthy cells. *p<0.05 versus control.

DISCUSSION

Osteosarcoma is the most common malignant bone tumor affecting all age groups. It exhibits a high propensity to develop metastases due to its rapid and aggressive proliferation, resulting in poor prognosis and treatment failure. Despite the expansion of research in this domain over the past decades, the invention of innovative therapies targeting the metastatic progression of osteosarcoma remains challenging. Therefore, it is crucial to deeply understand the molecular mechanisms of osteosarcoma to develop novel therapeutics targeting metastasis.[19] Metastasis encompasses several stages, including uncontrolled proliferation, increased cell migration, invasion, aggregation, and regulation of signalling pathways facilitating tumor progression.[20] Hence, the identification of compounds that may interfere with these processes serves as essential for formulating successful therapeutic strategies. In the present study, the antimetastatic potential of conessine in MG-63 osteosarcoma cells under TNF-α-induced inflammatory conditions, which mimic the TME, has been investigated using various *in vitro* assays. A comprehensive evaluation of the anti-metastatic potential of conessine assessed the distinct aspects of metastatic behaviour, including directional migration, collective cell migration, cell-cell interaction, and clonogenic survival.

The MTT assay revealed that conessine reduces MG-63 cell viability in a dose-dependent manner. Conessine, at higher doses, caused structural damage, including cell shrinkage, complete reduction of adherence, and formation of cellular debris. These morphological variations are consistent with cytotoxic stress and programmed cell death and correlated with the observed reduction in cell viability.[21] Phytochemicals from the family Apocynaceae possess potent anticancer activity, especially alkaloids and cardenolides, which inhibit cancer cell growth.[22] At higher concentrations, conessine, an alkaloid from Apocynaceae family, alters the mitochondrial activity and induces stress that leads to apoptosis.[23] Conessine exhibited cytotoxicity in MG-63 cells with an LC_{50} value of 154.83 µg/mL. Curcumin, one of the known phytochemicals used in anti-cancer products, exhibits the half-maximal inhibitory effect of 27.6 µM at 24 hr when applied to osteosarcoma cells.[24] Earlier studies reported that conessine exhibits cell proliferation, migration, and invasion efficacy in liver cancer cells.[23]

In this study, the antimetastatic efficacy of conessine on the osteosarcoma cell line was determined under the TME mimicked by TNF-α, which induces inflammatory conditions.[25] The simultaneous function of TNF-α as both a tumor necrosis factor and a tumor-promoting factor amplifies its metastatic potential. Thus, TNF-α inhibitors can be utilised to investigate osteosarcoma aggressiveness and pulmonary metastases in both *in vitro* and *in vivo* research.[25] Under the TNF-α-induced TME, conessine exhibited cytotoxicity on MG-63 cells with the LC_{50} value of 91.948 µg/mL. The LC_{50} value of conessine was lower in TNF-α-induced MG-63 cells compared to non-induced cells (154.83 µg/mL), indicating enhanced sensitivity of cells under inflammatory conditions. TNF-α stimulation mimics the TME by inducing cellular stress and inflammatory signaling, which may increase the vulnerability of cancer cells to therapeutic agents, suggesting that conessine may exhibit greater efficacy in targeting tumor cells under TME. The result of this assay showed that conessine reduces cell viability as well as attenuates the morphological

disruptions in TNF-α-induced MG-63 cells. This finding suggests that conessine may interfere with the stress-related signaling pathways activated by TNF-α and reduce the pathological cellular alterations while maintaining its cytotoxic action against cancer cells. Importantly, this effect indicates the efficacy of conessine in the normalization of TNF-α-induced cellular stress.

Migration of cancer cells through the ECM allows colonisation at distant sites, leading to metastasis.[26] TNF-α enhances the migratory effect of MG-63 cells, as demonstrated by a higher cell count (894 viable cells) on the transwell membrane compared to the control group (816 viable cells). This result aligns with prior reports demonstrating that inflammatory cytokines (TNF-α) can increase tumor cell motility and metastasis.[25] TNF-α stimulates pro-inflammatory signals that initially reduce cell motility; later, cancer cells activate NF-κB and other pro-inflammatory signalling mechanisms that support cytoskeletal reconstruction and migration.[27] Thus, anti-migration is one of the key strategies for preventing tumor metastasis. In the present study, conessine (91.948 µg/mL) effectively hindered the migration of osteosarcoma cells, as evidenced by fewer migrated cells (348 viable cells) than the untreated cells (894 viable cells), under TME. These findings revealed that conessine can reduce invasive and chemotactic migration even under inflammatory conditions. We observed effective anti-migration in MG-63 cells, which were not TNF-α-induced (124 viable cells). Phytochemicals are widely reported to inhibit the migration of cancer cells. For instance, ailanthone, a phytochemical derived from Chines medicinal plants, inhibited the migration of osteosarcoma cells in concentrations ranging from 0.2 to 0.4 µM. This study reported a significant reduction in stained cells on the membrane through microscopic images, not the quantitative assay.[28] Similar to the transwell assay, the scratch wound assay demonstrated that metastasis is strongly associated with increased cellular motility. The scratch wound assay conducted in this study demonstrated that control and TNF-α-induced MG-63 cells rapidly migrated to the wound area, leading to complete wound closure within 48 hr. However, the rate of wound closure in conessine-treated MG-63 cells was significantly reduced, and the wound remained open until 72 hr. Sun *et al*., demonstrated that curcumin treatment (10-20 µM) increases the wound area at 24 hr, from 46-88%.[24] The results of the above assays demonstrate the inhibition of collective cell migration by conessine on osteosarcoma cells, which is a critical step in metastatic dissemination.

The clonogenic assay measures the long-term proliferative and survival capacity of osteosarcoma cells. Enhanced colony formation stimulated by TNF-α leads to osteosarcoma progression by maintaining an undifferentiated state.[29] Conessine treatment intensely reduced the number of MG-63 colonies both in the presence (14 colonies) and absence (26 colonies) of TNF-α inflammation. Thymoquinone (0-50 µM), a natural product, significantly inhibited the survival of clonogenic triple-negative breast cancer cells, which were stimulated with TNF-α (50 ng/mL).[30] From the results of the cell viability and clonogenic assays, it has been determined that conessine not only inhibits immediate cell proliferation but also suppresses the ability of cancer cells to undergo long-term reproductive survival, a key property associated with metastasis.

Tumor cell aggregation strongly contributes to metastatic progression by enhancing the survival of circulating tumor cells and promoting tumor spheroid formation.[31] Microscopic images of the cell aggregation assay showed that MG-63 cells in both control and TNF-α-induced groups formed dense cell clusters after 48 hr. However, treatment using conessine markedly reduced aggregate formation and produced smaller, loosely organised

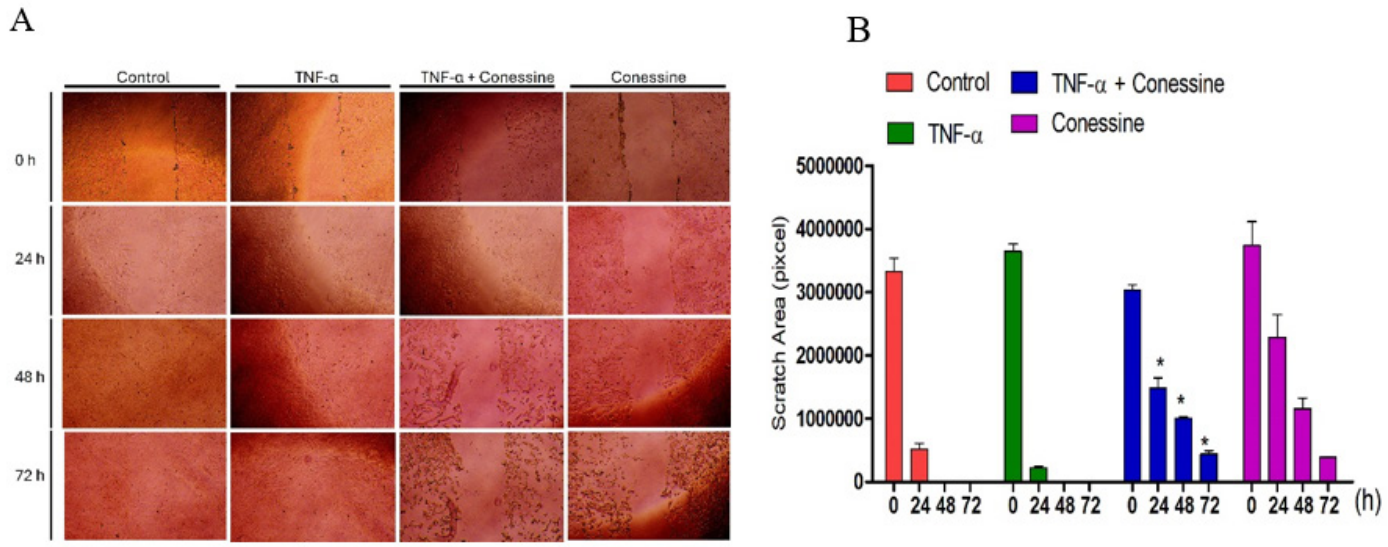

Figure 5: Effect of conessine on migration of osteosarcoma cells assessed by scratch wound healing assay. A-MRI-Images show wound closure of different experimental groups at varying incubation periods. B-Graphical representation illustrating a significant difference in wound closure recorded in different groups. *$p<0.05$ versus control.

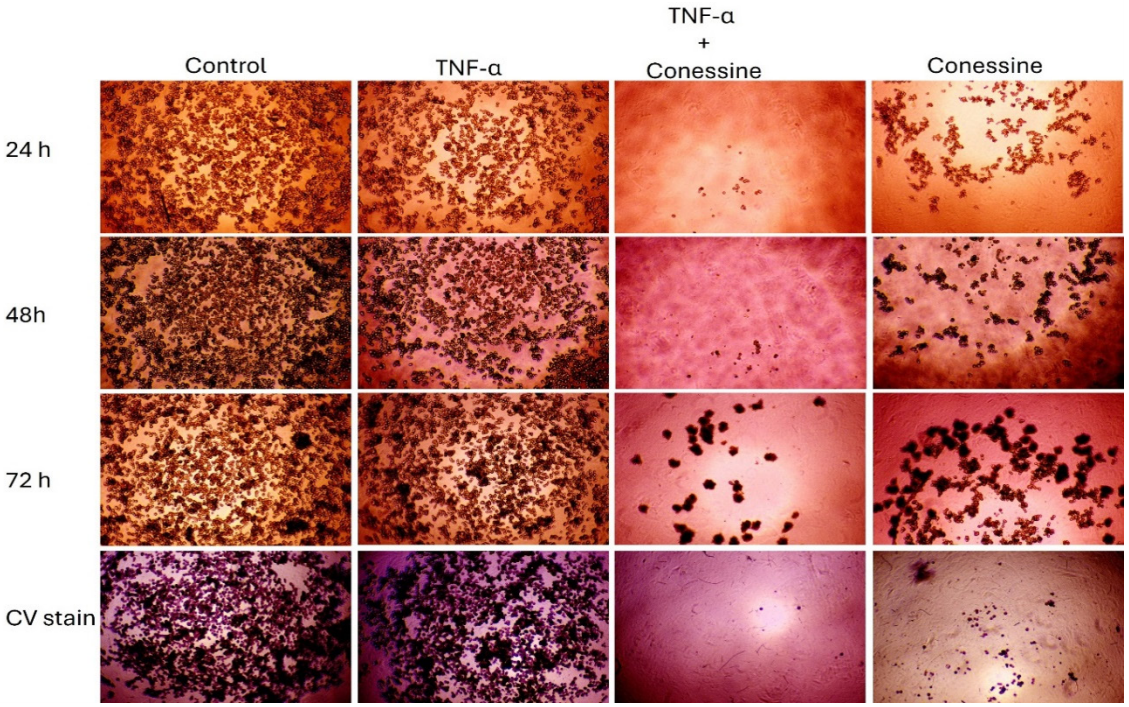

Figure 6: Effectiveness of conessine on the aggregation of osteosarcoma cells. Representative microscopic images showing aggregate formation at 24, 48, and 72 hr in control, TNF-α-treated, TNF-α + conessine-treated, and conessine-treated groups.

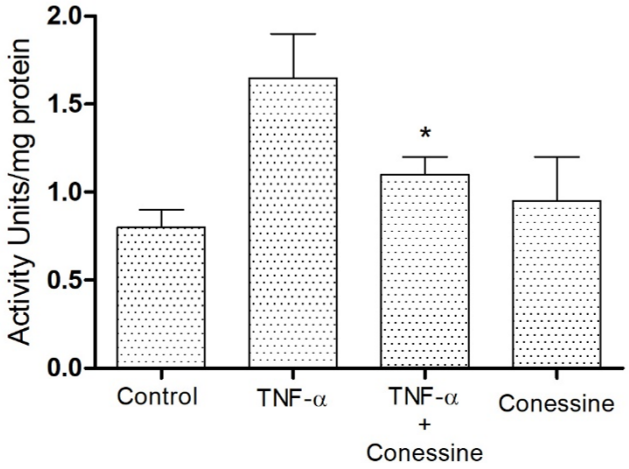

Figure 7: Indirect ELISA evaluated the expression of β-catenin in MG-63 osteosarcoma cells stimulated with TNF-α. Data are expressed as activity units per mg of protein. *p<0.05 versus TNF-α-induced.

clusters. TNF-α controls Epithelial-Mesenchymal Transition (EMT) and decreases adhesion molecules such as E-cadherin, thereby increasing cellular migration and metastatic activity in osteosarcoma and other solid tumors.[32] Conessine-treated cells exhibited impaired cell-cell adhesion and clustering.[33] Further investigation to find out the molecular mechanism underlying the above results, β-catenin expression was assessed using indirect ELISA. β-catenin is a key mediator of canonical Wnt signalling pathway, drives the cancer progression to proliferation, migration, EMT, and metastasis.[4] Our study demonstrated that TNF-α stimulation significantly increased β-catenin level in osteosarcoma cells, indicating the activation of Wnt/β-catenin signalling under inflammatory conditions.[4] Alkaloids have been claimed to suppress the Wnt/β-catenin signalling pathway and demonstrate potential anticancer activity in osteosarcoma cells. Evodiamine, a phytogenic alkaloid, suppress Wnt/β-catenin signalling system by modulating the expression of GSK-3β, which is a negative regulator of this pathway. Evodiamine enhances the expression level of TCF/LEF transcription factor, a primary nuclear mediator of canonical Wnt/β-catenin signalling, in osteosarcoma cells.[34] In our study, treatment with conessine reduced β-catenin activity in MG-63 cells, even under TME. This result suggests that the antimetastatic effects of conessine may be mediated through inhibition of the β-catenin signalling

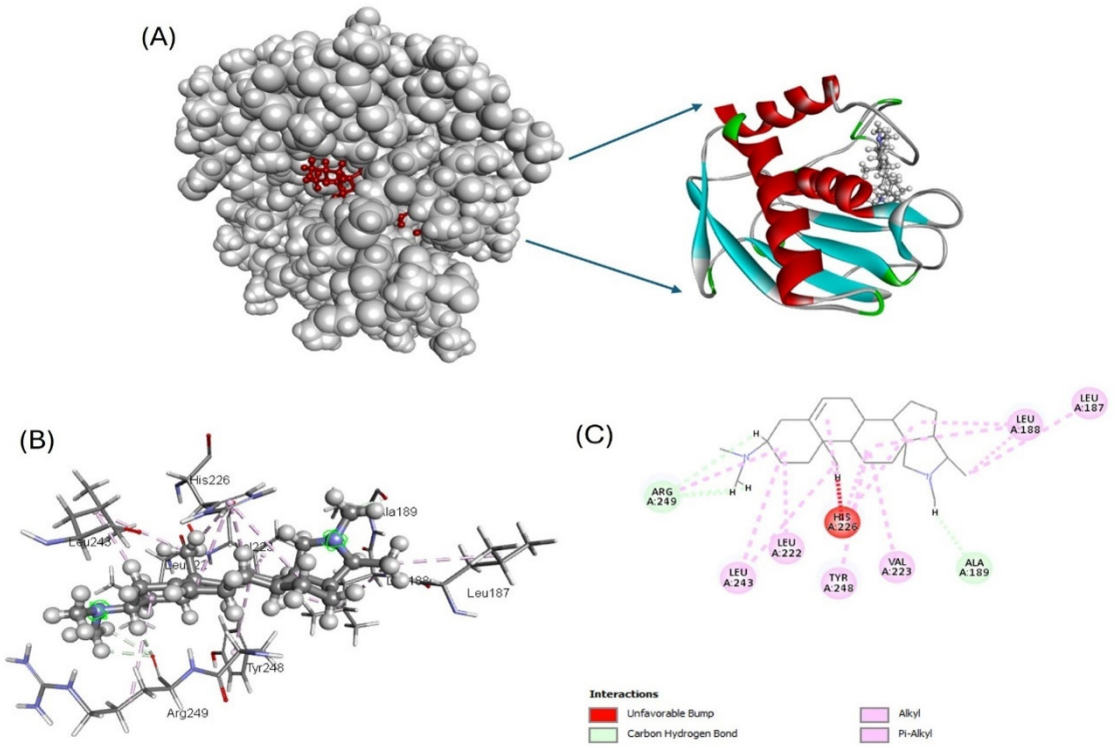

Figure 8: MMP9 Docking with conessine. (A) The surface representation of protein [PDB database (PDB ID: 6ESM)] ligand Complex; (B and C) Three and two-dimensional representation of the interaction between the ligand and the target.

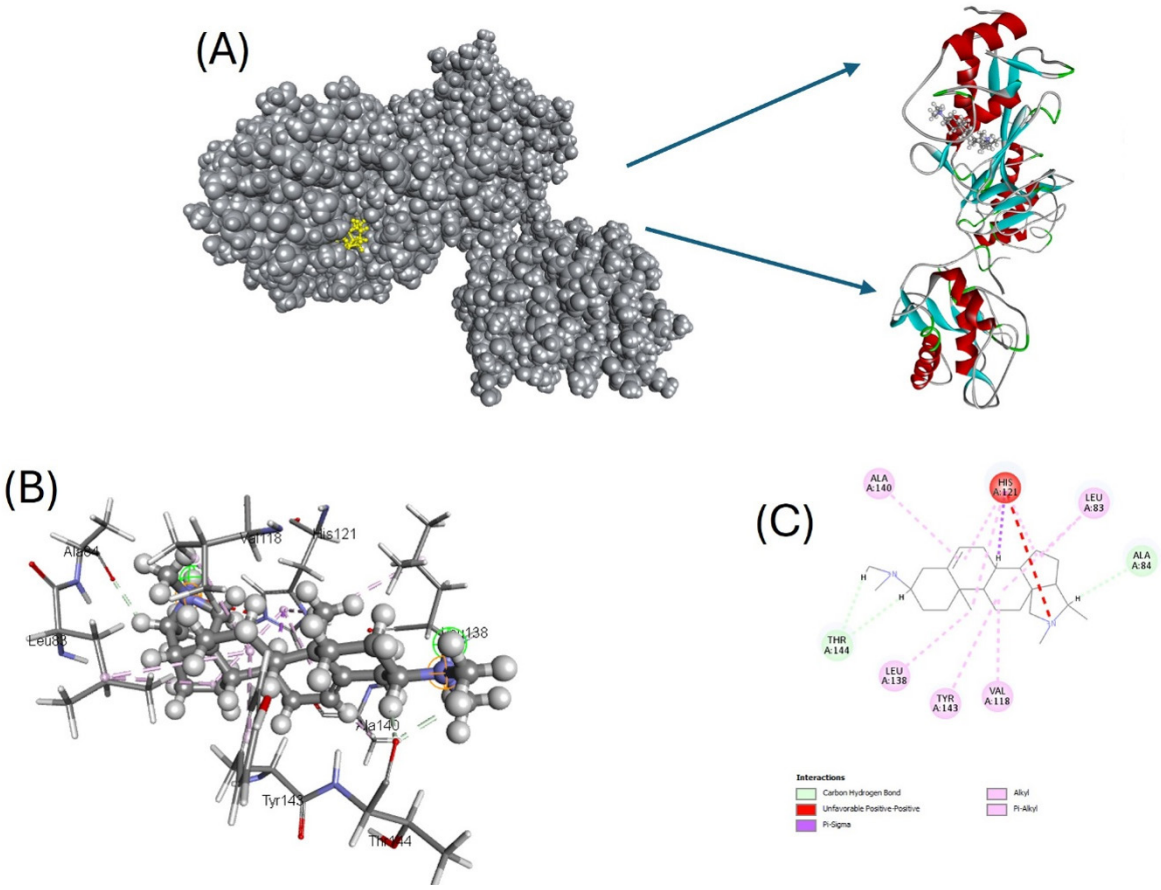

Figure 9: MMP2 Docking with conessine. (A) The surface representation of protein [PDB database (PDB ID: 7XGJ)] ligand Complex; (B and C) Three and Two-dimensional representation of the interaction between the ligand and the target.

pathway. Importantly, ELISA-based quantification provides relative protein expression level, further validation using Western blotting or gene expression analysis would be required to confirm β-catenin activity.

The degradation of the ECM in metastasis enables the tumor cells to invade and disseminate to distant tissues and organs due to the contribution of various proteolytic enzymes, especially MMPs. It has been proven that MMP2 and MMP9 mediate the degradation of type IV collagen, facilitating cancer cell migration and invasion. Overexpression of MMPs has been reported in osteosarcoma and is strongly associated with cell migration and metastatic spread. Hence, previous studies suggested that the establishment of MMP inhibitors not only inhibits osteosarcoma proliferation but also reduces metastatic spread of cancer to other organs.[35] In the present study, molecular docking analysis revealed that conessine binds with the catalytic domain of MMP9, exhibiting LibDock score of 130.527. The binding was stabilised by various hydrogen bonds (ALA189 and ARG249) along with a few hydrophobic (LEU187, LEU188, LEU222, LEU243, VAL223, HIS226, and TYR248) interactions. These interactions suggest that conessine may interfere with the enzymatic activity of MMP9. Ethone, a phytochemical from *Ageratum houstonianum*, showed stable interactions within the active site of MMP9.[36] The interacting residues were consistent with our docking report of MMP9, including LEU187, LEU188, LEU243, VAL223, and ARG249, suggesting that Conessine binds the catalytic binding pocket in a similar manner to known inhibitors. Similarly, conessine exhibited stable binding to MMP2, by achieving a LibDock score of 129.451. Alrumaihi demonstrated that the strong binding of drugs, CMNPD8322, CMNPD8320, and CMNPD8318, with MMP2 catalytic pocket residues including THR144, ALA84, LEU83, VAL118, ALA140, TYR143, and HIS12.[37] MMPs, particularly MMP2 and MMP9, play a significant role in osteosarcoma migration and invasion by degrading ECM components and facilitating metastasis.[38] However, when compared to the LibDock scores of reference inhibitor batimastat, conessine demonstrated lower values, indicating relatively poor binding affinity to MMPs. But considerable binding strength exhibited by conessine with the favourable residues suggests its stable interaction within the active site, so can act as a potent MMP inhibitor. While docking suggests potential interaction of conessine with MMP2 and MMP9, further biochemical and enzymatic assays are required to validate the direct inhibitory activity. The docking procedure is typically validated by redocking co-crystallized ligands and computing the Root Mean Square Deviation (RMSD). In these approaches, RMSD values of ≤ 2 Å are typically regarded as evidence of reliable docking efficacy. Although validation was not conducted in this study, the use of high-resolution crystal structures and the consistency of binding interactions with reported active-site residues strengthen the credibility of the docking results. Subsequent research will include RMSD-based validation and redocking methodologies to enhance the confirmation of docking precision.[39]

In the present study, multiple assays were employed to evaluate the efficacy of conessine on different, complementary aspects of metastatic behaviour. Transwell analysis demonstrated a considerable inhibition of cancer cell migration following conessine treatment, indicating decreased invasive potential. The scratch assay results showed sustained inhibition of wound closure up to 72 hr, confirming reduced proliferation. The aggregation assay revealed impaired cell-cell interaction and the clonogenic assay showed a significant reduction in long-term survival and anchorage-independent growth capacity of cancer cells. Molecular docking analysis conducted in the present study revealed that conessine binds to the catalytic domain of both MMPs, thereby interfering with their enzymatic activities in metastasis. Our experimental findings demonstrated that reduced migration/invasion and modulation of metastatic markers are consistent with possible MMP inhibition.[40] The docking results are presented as supportive, hypothesis-generating evidence rather than definitive proof of target engagement. ECM modelling involves contributions from clonogenic survival and cell aggregation,[41] both of which were also inhibited by conessine. Additionally, conessine's inhibition of the β-catenin signalling, recognised as a metastasis-related pathway, influences the MMP expression.[42] These findings collectively provide a multi-dimensional evaluation of the anti-metastatic efficacy of conessine.

CONCLUSION

The present study demonstrates that conessine, a natural steroid alkaloid, has been proven to possess potential antimetastatic properties against MG-63 osteosarcoma cells. Conessine inhibited osteosarcoma cell viability, migration, and colony formation under inflammatory conditions, demonstrating its antiproliferative effects. Reduction in β-catenin expression suggests that conessine may suppress signalling pathways involved in tumor progression and metastasis. Molecular docking studies further supported the above findings by revealing the effective binding of conessine to MMPs, a metastasis-associated enzyme. Overall, this study suggests that conessine exhibits promising anti-metastatic activity against osteosarcoma, and additional research, including molecular dynamics, formulation studies, and *in vivo* validation, is required to elucidate the underlying mechanisms and further develop conessine's clinical significance.

ACKNOWLEDGEMENT

None.

ABBREVIATIONS

ANOVA: Analysis of Variance; **ATCC:** American Type Culture Collection; **BM:** Basement Membrane; **CCD:** Charge-Coupled Device; **CHARMM:** Chemistry at HARvard Macromolecular Mechanics; **CO_2:** Carbon Dioxide; **DMEM:** Dulbecco's Modified Eagle's Medium; **DMSO:** Dimethyl Sulfoxide; **DNA:** Deoxyribonucleic Acid; **ECM:** Extracellular Matrix; **ELISA:** Enzyme-Linked Immunosorbent Assay; **EMT:** Epithelial-Mesenchymal Transition; **FBS:** Fetal Bovine Serum; **GLN:** Glutamine; **GSK-3β:** Glycogen Synthase Kinase-3 Beta; **HIV:** Human Immunodeficiency Virus; **HRP:** Horseradish Peroxidase; **IC_{50}:** Half Maximal Inhibitory Concentration; **LC_{50}:** Lethal Concentration 50; **LEF:** Lymphoid Enhancer-Binding Factor; **LibDock:** Ligand Docking Algorithm; **MG-63:** Human Osteosarcoma Cell Line; **MI:** Michigan; **MMP:** Matrix Metalloproteinase; **MMP-2:** Matrix Metalloproteinase-2; **MMP-9:** Matrix Metalloproteinase-9; **MTT:** 3-(4,5-Dimethylthiazol-2-yl)-2,5-Diphenyl Tetrazolium Bromide; **NF-κB:** Nuclear Factor Kappa-B; **OD:** Optical Density; **PBS:** Phosphate Buffered Saline; **PDB:** Protein Data Bank; **PI3K:** Phosphoinositide 3-Kinase; **RCSB-PDB:** Research Collaboratory for Structural Bioinformatics Protein Data Bank; **SD:** Standard Deviation; **SE:** Standard Error; **STAT3:** Signal Transducer and Activator of Transcription 3; **TCF:** T-Cell Factor; **TME:** Tumor Microenvironment; **TNF-α:** Tumor Necrosis Factor Alpha; **UV-vis:** Ultraviolet-visible Spectrophotometry; **Wnt:** Wingless-Related Integration Site Signaling Pathway.

CONFLICT OF INTEREST

The authors declare that there is no conflict of interest.

FUNDING

There is no funding received for this research.

ETHICAL STATEMENT

Not applicable

AUTHOR CONTRIBUTIONS

All research and writing has been equally contributed by both authors.

SUMMARY

This study investigated the anti-proliferative and anti-metastatic potential of conessine, a steroidal alkaloid, against MG-63 human osteosarcoma cells under TNF-α-induced inflammatory conditions. Cytotoxicity analysis using the MTT assay demonstrated dose-dependent inhibition of cell viability with LC_{50} values of 154.83 µg/mL in normal MG-63 cells and 91.94 µg/mL in TNF-α-stimulated cells. Functional assays, including transwell migration, scratch wound healing, clonogenic, and aggregation assays, revealed that conessine significantly suppressed cell migration, colony formation, and metastatic behavior. Conessine also reduced β-catenin activity, indicating inhibition of the Wnt/β-catenin pathway. Molecular docking further showed stable binding of conessine with metastasis-associated enzymes MMP-2 and MMP-9, supporting its potential as a promising anti-metastatic therapeutic candidate for osteosarcoma.

REFERENCES

1. Wang Y, Zhang H, Yao P, Teng S. Linking Environmental Hazards to Osteosarcoma Development: A Comprehensive Review. Cancer Management and Research. 2025: 1725-39.
2. Alduraibi KA, Towhari JA, Alebdi HA, Alfadhel BZ, Alotaibi GS, Ghosh S, *et al.* Osteosarcoma metastasis to the thorax: A pictorial review of chest computed tomography findings. Diagnostics. 2024;14(18):2085.
3. Song Z, Wang J, Su Q, Luan M, Chen X, Xu X. The role of MMP-2 and MMP-9 in the metastasis and development of hypopharyngeal carcinoma. Brazilian Journal of Otorhinolaryngology. 2021;87(5):521-8.
4. Sun L, Xing J, Zhou X, Song X, Gao S. Wnt/β-catenin signalling, epithelial-mesenchymal transition and crosslink signalling in colorectal cancer cells. Biomedicine & Pharmacotherapy. 2024;175:116685.
5. Beg S, Handa M, Shukla R, Rahman M, Almalki WH, Afzal O, *et al.* Wearable smart devices in cancer diagnosis and remote clinical trial monitoring: Transforming the healthcare applications. Drug discovery today. 2022;27(10):103314.
6. Patrice BK, Véronique PB, David L, François-Xavier E. Antibacterial activities of the extracts and conessine from Holarrhena floribunda G. Don.(Apocynaceae). African Journal of Traditional, Complementary, and Alternative Medicines. 2007;4(3):352.
7. Abdulkareem AH, Alani MT, Awad SA, Al-Meani SAL, Ahmed MM, Abdulkareem EH, *et al.* Dual Inhibitory Potential of Conessine Against HIV and SARS-CoV-2: Structure-Guided Molecular Docking Analysis of Critical Viral Targets. Viruses. 2025;17(11):1435.
8. Zhang S, Ren H, Sun H, Cao S. Dieckol exerts anticancer activity in human osteosarcoma (MG-63) cells through the inhibition of PI3K/AKT/mTOR signaling pathway. Saudi Journal of Biological Sciences. 2021;28(9):4908-15.
9. Baig MNu, Alvi SB, Alvala M, *et al.* Ranolazine as a protective agent against Lung Cancer: A translational approach. Asian Journal of Pharmaceutical and Health Sciences. 2020;10(1):2224-2230. doi:10.5530/1pxc8696
10. Arunachalam K, Sreeja PS. MTT assay protocol. Advanced cell and molecular techniques: protocols for *in vitro* and *in vivo* studies: Springer; 2025. p. 271-6.
11. Pacheco FJ, Almaguel FG, Evans W, Rios-Colon L, Filippov V, Leoh LS, *et al.* Docosahexanoic acid antagonizes TNF-α-induced necroptosis by attenuating oxidative stress, ceramide production, lysosomal dysfunction, and autophagic features. Inflammation research. 2014;63(10):859-71.
12. Justus CR, Leffler N, Ruiz-Echevarria M, Yang LV. *In vitro* cell migration and invasion assays. Journal of visualized experiments: JoVE .2014(88):51046.
13. Brix N, Samaga D, Belka C, Zitzelsberger H, Lauber K. Analysis of clonogenic growth *in vitro*. Nature protocols. 2021;16(11):4963-91.
14. Martinotti S, Ranzato E. Scratch wound healing assay. Epidermal cells: methods and protocols: Springer; 2019. p. 225-9.
15. Santambrogio A, Horne RI, Metrick MA, Gallagher NC, Brotzakis ZF, Rinauro D, *et al.* Design of Tau aggregation inhibitors using iterative machine learning and a polymorph-specific brain-seeded fibril amplification assay. Journal of the American Chemical Society. 2025;147(39):35942-52.
16. Surendran S, Suresh G, Vijayakumar N, Ramachandran R. Autophagy and Parkinsons disease-role of caffeine as autophagic stimulator and anti apoptotic agent. Nepal Journal of Biotechnology. 2023;11(2):57-64.
17. Bradford MM. A rapid and sensitive method for the quantitation of microgram quantities of protein utilizing the principle of protein-dye binding. Analytical biochemistry. 1976;72(1-2):248-54.
18. Diller DJ, Li R. Kinases, homology models, and high throughput docking. Journal of medicinal chemistry. 2003;46(22):4638-47.
19. Sheng G, Gao Y, Yang Y, Wu H. Osteosarcoma and metastasis. Frontiers in oncology. 2021;11:780264.
20. Li Y, Liu F, Cai Q, Deng L, Ouyang Q, Zhang XH-F, *et al.* Invasion and metastasis in cancer: molecular insights and therapeutic targets. Signal transduction and targeted therapy. 2025;10(1):57.
21. Kari S, Subramanian K, Altomonte IA, Murugesan A, Yli-Harja O, Kandhavelu M. Programmed cell death detection methods: a systematic review and a categorical comparison. Apoptosis. 2022;27(7):482-508.
22. Wong SK, Chan HT, Chan EWC. Chemistry, resources, anticancer effects, other pharmacological properties, and clinical trials of oleandrin from Nerium oleander: An overview. Journal of Applied Pharmaceutical Science. 2025;15(12):004-12.
23. Li C-Y, Lin Y-S. Conessine inhibits cell proliferation, migration and invasion, and induces apoptosis in liver cancer cells. Cancer Research. 2024; 84(6_Supplement):1821.

24. Sun Y, Liu L, Wang Y, He A, Hu H, Zhang J, *et al.* Curcumin inhibits the proliferation and invasion of MG-63 cells through inactivation of the p-JAK2/p-STAT3 pathway. OncoTargets and therapy. 2019: 2011-21.
25. Khan S, Aldawood Y, Shaikh AH, Zobairi A, Nabilah U, Alqahtani H, *et al.* Tumor necrosis factor-alpha's role in the pathophysiology of colon cancer Diseases. 2025;13(6):185.
26. Xue J, Yang X-r, Wang L. NF-κB signaling pathway in osteosarcoma: from signaling networks to targeted therapy. Frontiers in Oncology. 2025;15:1565760.
27. Li R, Wen A, Lin J. Pro-inflammatory cytokines in the formation of the pre-metastatic niche. Cancers. 2020;12(12):3752.
28. Zhang Y, Gong R, Liu Y, Sun X, Liang J, Zhou Y, *et al.* Ailanthone inhibits proliferation, migration and invasion of osteosarcoma cells by downregulating the serine biosynthetic pathway. Frontiers in Oncology. 2022;12:842406.
29. Mori T, Sato Y, Miyamoto K, Kobayashi T, Shimizu T, Kanagawa H, *et al.* TNFα promotes osteosarcoma progression by maintaining tumor cells in an undifferentiated state. Oncogene. 2014;33(33):4236-41.
30. Adinew GM, Messeha S, Taka E, Mochona B, Redda KK, Soliman KF. Thymoquinone inhibition of chemokines in TNF-α-induced inflammatory and metastatic effects in triple-negative breast cancer cells. International journal of molecular sciences. 2023;24(12):9878.
31. Arora S, Singh S, Mittal A, Desai N, Khatri DK, Gugulothu D, *et al.* Spheroids in cancer research: Recent advances and opportunities. Journal of Drug Delivery Science and Technology. 2024;100:106033.
32. Zhang R, Zhou X, Shen C. Inflammation-driven prognostic model and immune landscape profiling in osteosarcoma. Discover Oncology. 2025;16(1):2061.
33. Sharma V, Chaudhary AA, Bawari S, Gupta S, Mishra R, Khan S-U-D, *et al.* Unraveling cancer progression pathways and phytochemical therapeutic strategies for its management. Frontiers in Pharmacology. 2024;15:1414790.
34. Yang S, Chen J, Tan T, Wang N, Huang Y, Wang Y, *et al.* Evodiamine exerts anticancer effects against 143B and MG63 cells through the Wnt/β-catenin signaling pathway. Cancer management and research. 2020: 2875-88.
35. Doppelt-Flikshtain O, Asbi T, Younis A, Ginesin O, Cohen Z, Tamari T, *et al.* Inhibition of osteosarcoma metastasis *in vivo* by targeted downregulation of MMP1 and MMP9. Matrix Biology. 2024;134:48-58.
36. Verma A, Rizvi SMD, Shaikh S, Ansari MA, Shakil S, Ghazal F, *et al.* Compounds isolated from Ageratum houstonianum inhibit the activity of matrix metalloproteinases (MMP-2 and MMP-9): An oncoinformatics study. Pharmacognosy Magazine. 2014;10(37):18.
37. Alrumaihi F. A cheminformatics-biophysics correlate to identify promising lead molecules against matrix metalloproteinase-2 (MMP-2) enzyme: A promising anti-cancer target. Saudi Pharmaceutical Journal. 2023;31(7):1244-53.
38. Shoari A, Ashja Ardalan A, Dimesa AM, Coban MA. Targeting invasion: the role of MMP-2 and MMP-9 Inhibition in colorectal cancer therapy. Biomolecules. 2024;15(1):35.
39. Saeed M, Siddiqui S, Tasleem M, Alam MJ, Alqathani SS, Bardakci F, Almuzaini N, Upadhyay TK, Abdalla RA, Aqil F. *In silico* analysis of plumbagin's interaction with caspase 9: unveiling its potential as an anti-NSCLS agent. Journal of Biomolecular Structure and Dynamics. 2026;44(1):26-36.
40. Song J, Zhao T, Wang C, Sun X, Sun J, Zhang Z. Cell migration in diabetic wound healing: Molecular mechanisms and therapeutic strategies. International Journal of Molecular Medicine. 2025;56(2):126.
41. Crossley RM, Johnson S, Tsingos E, Bell Z, Berardi M, Botticelli M, *et al.* Modeling the extracellular matrix in cell migration and morphogenesis: a guide for the curious biologist. Frontiers in cell and developmental biology. 2024;12:1354132.
42. Deldar Abad Paskeh M, Mirzaei S, Ashrafizadeh M, Zarrabi A, Sethi G. Wnt/β-catenin signaling as a driver of hepatocellular carcinoma progression: an emphasis on molecular pathways. Journal of Hepatocellular Carcinoma. 2021: 1415-44.

Cite this article: Makeen HA, Albratty M. Anti-Proliferative and Anti-Metastatic Effects of Conessine in Human Osteosarcoma Cells: In vitro and in silico Evidence Targeting MMP2 and MMP9 . Indian J of Pharmaceutical Education and Research. 2026;60(4):1681-95.